Article:
Cain, R, Salimraj, R, Punekar, AS et al. (8 more authors) (2019) Structure-Guided Enhancement of Selectivity of Chemical Probe Inhibitors Targeting Bacterial Seryl-tRNA Synthetase. Journal of Medicinal Chemistry, 62 (21). pp. 9703-9717. ISSN 0022-2623

https://doi.org/10.1021/acs.jmedchem.9b01131

Structure-guided enhancement of selectivity of chemical probe inhibitors targeting bacterial seryl-tRNA synthetase (SerRS)

Ricky Cain,[a]+ Ramya Salimraj,[a]+ Avinash S. Punekar,[a] Dom Bellini,[a] Colin W. G. Fishwick ,[b] Lloyd Czaplewski,[c] David J. Scott,[d,e] Gemma Harris[e], Christopher G. Dowson,[a] Adrian J. Lloyd,[a] David I. Roper[a]

[a] School of Life Sciences, University of Warwick, Gibbet Hill Road, Coventry, CV4 7AL, United Kingdom.

[b] School of Chemistry, University of Leeds, Leeds, LS2 9JT, United Kingdom.

[c] Chemical Biology Ventures Limited, Abingdon, OX14 1XD, United Kingdom

[d] School of Biosciences, University of Nottingham, Nottingham, LE12 5RD, United Kingdom

[e] ISIS Spallation Neutron and Muon Source and the Research Complex at Harwell, Rutherford Appleton Laboratory, Oxfordshire OX11 0FA, United Kingdom

+ These authors contributed equally to this work

E-mail: david.roper@warwick.ac.uk

Abstract

Aminoacyl-tRNA synthetases are ubiquitous and essential enzymes for protein synthesis and also a variety of other metabolic process especially in bacterial species. Bacterial Aminoacyl-tRNA synthetases represent attractive and validated targets for antimicrobial drug discovery if issues of prokaryotic verses eukaryotic selectivity and antibiotic resistance generation can be addressed. We have determined high resolution X-ray crystal structures of the E. coli and S. aureus seryl-tRNA synthetases in complex with amino-acyl adenylate analogues and used computational drug discovery techniques to explore a class of small molecule inhibitors that selectively bind the bacterial seryl-tRNA synthetases over their human homologues, opening a route to selective chemical inhibition of these bacterial targets.

Introduction

The fidelity of protein synthesis is absolutely reliant upon the provision of specific amino acids by tRNA molecules for use by the ribosome.[1] Errors in this process lead to defects in protein folding and function leading to cell death.[2] Each of the 20 amino acids has its own aminoacyl-tRNA synthetase (aaRS) which catalyses the attachment of the amino acid to its cognate tRNA. Despite the fact that all aaRSs share the same overall mechanism it has long been recognised there is clearly significant diversity between bacterial, mammalian and archaeal enzymes to allow for synthetic and natural product discrimination between pathogen and host enzymes[3-5]. In addition, several amino acids are able to bind non-cognate aaRSs allowing for the possibility of exploiting this feature for antimicrobial discovery. For example, the amino acid serine is able to bind the alanyl-(AlaRS), and threonyl-tRNA synthetase (ThrRS) along with its cognate seryl-tRNA synthetase (SerRS)[6]. This incorrect binding is rectified in nature by numerous proofreading mechanisms[7, 8]. However, in this context one of the major challenges presented by aaRS as targets for antimicrobial drug discovery, is their ubiquitous presence in organisms and particularly with respect to bacterial infection in human tissues requiring exploration of strategies that allow for bacterial selectivity to prevent issues of specificity and toxicity[9].

Aminoacyl sulfamoyl adenosines (aaSAs) are non-hydrolysable mimetics of the aminoacyl adenylate intermediate (aaAMP) formed during the aaRS catalytic cycle and are potent inhibitors of these enzymes.[10] A significant number of natural product inhibitors mimic these reaction intermediates forming tight binding complexes with substantial affinity competing effectively with natural substrates. Of those, mupirocin is the most prominent example which has found clinical utility as a topic treatment for soft tissue infections. Mupirocin targets the IleRS enzyme and utilises a hydrophobic "tail" in addition to aminoacyl adenylate warhead to bind to its target[11]. By contrast to many antibiotics in clinical use, seryl sulfamoyl adenosine (SerSA, **1**) can bind and inhibit AlaRS and ThrRS in addition to SerRS and hence is a multi-targeting inhibitor[6, 12]. It can be predicted therefore that SerSA would therefore require mutations in several of these enzymes before a resistance phenotype could be conferred.

Although the X-ray crystal structure of E.coli SerRS[13] was solved in 1990 and several further related reports have been published, on SerRS from T. thermophilus[14, 15], Methanosarcina barkeri[16], Pyrococcus horikoshii[17], Candida albicans[18] as well as human cytoplasmic[19] and bovine mitochondrial[20] form of the protein, there are no entries for E.coli SerRS in the protein databank hampering efforts in antimicrobial structure guided drug discovery. Moreover, the X-ray crystal structure of Human Seryl-tRNA Synthetase and Ser-SA complex reveals specific conformational changes upon catalysis necessary for function which are not found in bacterial homologues providing further perspectives upon changes in structure that may

allow prokaryotic from eukaryotic specificity.[19] In this study we set out to increase the available structural information for human bacterial pathogens and use this to investigate the possibilities for designing bacterial specific SerRS enzyme inhibitors.

Results

Crystal structures of SerRS in complex with SerSA.

The electron density maps of the crystal structures of full-length SerRS from Escherichia coli and Staphylococcus aureus complexed with SerSA at 1.98 Å and 2.03 Å, respectively (**Fig. 1**, **Supplementary Table 1**), were unambiguous for SerSA. In both structures, SerSA bound deep into a well-conserved SerRS aminoacylation catalytic pocket and stabilized by a network of hydrogen bond interactions from the residues in motif 2, motif 3 and the serine-binding TxE motif (Fig. 1A) - a typical binding mode in all class 2 aaRS. Superimposition of the SerSA bound structures of E. coli, S. aureus and human cytoplasmic SerRS (PDB ID: 4L87[19]) shows a high degree of similarity between the active site pockets and the orientations of the bound SerSA. However, the N-terminal tRNA-binding domain (i.e. the two-stranded anti-parallel coiled coil making the long helical arm) protruding away from the active site pockets in the compared structures shows large conformational changes resulting in a high RMSD (**Supplementary Table 2**). The purine ring of the adenosine in SerSA is sandwiched between a conserved phenylalanine (F287 in E. coli SerRS, F281 in S. aureus SerRS and F321 in human cytoplasmic SerRS) and arginine (R397 in E. coli SerRS, R391 in S. aureus SerRS and R435 in human cytoplasmic SerRS), showing a typical π–π stacking interaction (Fig. 1B). The M284 in E. coli SerRS, L278 in S. aureus SerRS and V318 in human cytoplasmic SerRS play a same role by providing adenosine specificity through two main chain hydrogen bond interactions with the ring nitrogen's (Fig. 1C). The 2'-OH and the 3'-OH of the ribose ring in SerSA interact with the carbonyl oxygen of a hydrophobic residue (I356 in E. coli SerRS, I350 in S. aureus SerRS and L392 in human cytoplasmic SerRS) and a conserved glutamic acid (E355 in E. coli SerRS, E349 in S. aureus SerRS and E391 in human cytoplasmic SerRS) respectively. The seryl moiety of SerSA extends deep into the pocket to interact with T237, E239, R268, E291, N389 and S391 in E. coli SerRS and equivalent residues in S. aureus SerRS and human cytoplasmic SerRS.

Design and synthesis of the selectivity probe.

The X-ray crystal structures of E. coli SerRS, S. aureus SerRS and the human cytoplasmic SerRS (PDB ID: 4L87) were overlaid in Maestro.[21] Interestingly, a thorough analysis of the active site pockets revealed a small extension in the hydrophobic cavity adjacent to the C-2 position of SerSA in the E. coli and S.

aureus SerRS structures (**1**). This hydrophobic cavity extension is absent in the human cytoplasmic SerRS (**Supplementary Fig. 1b**) as it is filled by the bulkier side-chain of T434.

A focussed structure activity relationship (SAR) series with variants of the C-2 position of SerSA adenosine was designed to investigate the steric tolerance of the hydrophobic cavity and to establish the degree of selectivity for the bacterial over the human cytoplasmic SerRS (**Fig. 2a**). In silico molecular docking of the designed selectivity probes into the active site pockets of the E. coli, S. aureus and human cytoplasmic SerRS crystal structures (**Supplementary Methods**) and visual analysis of the predicted docking poses (**Supplementary Fig. 1c-d**) suggested that chloro- and iodo-seryl sulfomyl adenylate derivatives **2** and **3** respectively would not achieve selectivity with **2** and **3** are predicted to interact equally as well with both the bacterial and human cytoplasmic SerRS. Compounds **4-8** were however predicted to exhibit selectively for the bacterial SerRS over the human SerRS.

The bulkier groups located at the 2 position of compounds **4-8** were predicted to be accommodated in the pocket of the bacterial enzymes. However, due to the steric hindrance from the T434 residue in the human cytoplasmic SerRS, compounds **4-8** were predicted to change the torsional angle between the adenine and ribose sugar upon binding to the human cytoplasmic SerRS. As a result of the torsional change the π-π stacking interactions with F287 and the backbone interaction to V318 are lost leading to a weaker predicted binding affinity and therefore increased selectivity for the bacterial SerRS (**Supplementary Fig. 1d**).

Preparation of SerSA selectivity probes was initiated by the acid-catalysed protection of the commercially available 2-chloroadenosine or 2-iodoadenosine (Fluorochem, UK) to provide the acetyl-protected adenosines (95-97%)(**Supplementary Synthesis**). A Suzuki coupling reaction between the protected adenosine and desired boronic acid species (20-70%) was conducted,[22] before sulfonation using sulfonyl chloride to afford the sulfonamide (90-95%). The sulfonamide was then coupled to the succinimide activated protected serine **(S1, Supplementary information)** to yield the protected product (40-50%). Removal of the benzyl group was accomplished by treatment with a solution of boron trichloride dimethyl sulfide complex (2M in DCM),[23] and the resulting alcohol was treated with trifluoroacetic acid and water to yield compounds **2-8** (**2-8**, see **Experimental Section** and **Supplementary Information** for details).

Bacterial synthetase inhibition by selectivity probe

Using a continuous, spectrophotometric assay that specifically measures the adenylate formation reaction[6], compounds **2-8** were evaluated for inhibition of the ATP dependent aminoacyl adenylate in the E. coli SerRS and S. aureus SerRS enzymes and compared to the inhibition of the parent seryl adenylate, compound **1**. Our analysis reveals compounds **2-8** to be active against E. coli SerRS and S. aureus SerRS with IC_{50} values ranging from 378 nM to 52.7 μM (**Table 1**). Compound **2** exhibited sub micromolar

inhibition of the S. aureus SerRS and E. coli SerRS with IC_{50}s of 262 nM and 445 nM respectively. Compound **3** also exhibited sub-micromolar inhibition of S. aureus SerRS with an IC_{50} of 378 mM but weaker inhibition against E. coli SerRS with an IC_{50} of 1.36 µM. Compounds **4-8** all manifested low micromolar inhibition against both E. coli and S. aureus SerRS as detailed in table 1. A general trend is observed where increasing the size of the group at the 2 position of the adenylate decreases the binding affinity to the bacterial synthetase. Alanyl sulfamoyl adenosine (AlaSA, **9**) and threonyl sulfamoyl adenosine (ThrSA **10**) were also evaluated for inhibition against E. coli SerRS and S. aureus SerRS (**Supplementary Table 5**). AlaSA **9** showed no inhibitory activity against either enzyme at 1 mM while **10** manifested IC_{50}s of 285 µM and 231 µM against E. coli SerRS and S. aureus SerRS respectively, thus exhibiting much weaker binding than the designed selectivity probes. This result highlights the key nature of the beta-hydroxyl of the serine to the overall binding of the compound to the adenylate formation site in these enzymes and that overall inhibitory properties of Seryl adenylate inhibitors modified around the C-2 position of the SerSA adenosine.

Human synthetase inhibition by selectivity probes

Measurement of the IC_{50} inhibition kinetics of the original Seryl adenylate, compound **1** against the bacterial and human SerRS enzymes, reveals a 10-fold difference overall, in favour of greater specificity for the inhibitor towards the bacteria enzymes. Compounds **2-8** were subsequently screened for inhibition of the human cytoplasmic SerRS (**Table 1**) using the same assay system. Assay measurements of compounds **2** and **3,** revealed a 31-fold and 11-fold increase in IC_{50} against the bacterial and human enzymes**,** indicating compounds **2** and **3** were not exhibiting selectivity overall and had lower affinity than the original adenylate, compound **1**. Overall the observed IC_{50} of compounds 2-8 increased with respect to the parental adenylate but remarkably inhibition of the human cytoplasmic SerRS was effectively abolished in compounds **4-8** with IC_{50} values greater than 1 mM, revealing significant selectivity of these compounds towards the tested bacterial seryl synthetases. The best of these compounds (**7**), with a 3-Thienyl at the C-2 position of the SerSA adenosine had an increase in IC_{50} over the parent compound **1** of 6.8 and 8.4 fold for E. coli and S. aureus enzymes respectively, with effectively negligible binding to the human homologue. The observed selectivity overall was attributed to the increased size of **4-8** making them unable to fit into the hydrophobic pocket located in the human cytoplasmic SerRS active site due to the presence of T434 as previously hypothesised.

Binding studies of E. coli SerRS with SerSA and derivative 8

The binding stoichiometry and affinity of SerSA **1** and compound **8** to E. coli SerRS was determined using isothermal titration calorimetry (ITC). Titration of SerSA to E. coli SerRS resulted in a steep slope in the

binding isotherm suggesting a very tight binding of the inhibitor to the enzyme. Interestingly, fitting of this binding isotherm using a single site model showed a 2:1 SerSA:SerRS stoichiometry with an overall dissociation constant K_d = 1.27 nM (**Supplementary Fig. 4a**). The combination of very high affinity and low enthalpy unfortunately prevented an accurate measurement of K_d for SerSA at the individual binding sites.

By contrast, titration of compound **8** to E. coli SerRS resulted in a binding isotherm (2:1 compound **8**:SerRS stoichiometry) that after fitting using a two independent sites model clearly showed two distinct binding sites with dissociation constants K_{d1} = 0.29 µM and K_{d2} = 1.92 µM (**Supplementary Fig. 4b**). As $K_{d2} > 4$ K_{d1}, there is apparent mild negative cooperativity within the system. In both experiments, a negative enthalpy value detected for such a tight interaction indicates the role of hydrogen bond and electrostatic interactions in the stabilisation of the enzyme–inhibitor complex. The observation of two binding sites for SerSA and compound 8 prompted us to investigate the oligomeric state of the E. coli SerRS in solution which are typically dimers in solution.[24] Analytical ultracentrifugation (AUC) experiments were carried out with E. coli SerRS to confirm the oligomeric state of the protein in the presence and absence of SerSA and **8 (Supplementary Table 6)**. The results confirmed E. coli SerRS, both with and without either ligand, appeared with a molecular weight that is consistent with a dimer in solution (**Supplementary Fig. 3**). The observed SerSA and compound **8** binding stoichiometry is consistent with the previous structural findings showing two SerSA molecules bound to two distinct sites in Candida albicans SerRS (PDB ID: 3QO8)[25]. However, in the Candida albicans SerRS the second, largely hydrophobic adenylate binding site described in the X-ray crystal structure is located 26 Å distant from the active site and appears to play no role in enzyme function or protein-protein interaction as described by the authors [25].

Structural basis of selectivity probe binding to E. coli SerRS

To understand the molecular basis of the selectivity probe towards a bacterial SerRS we attempted a series of co-crystallisation and compound soaking experiments using unliganded E. coli or S. aureus SerRS. Despite an extensive search of conditions to co-crystallise S. aureus SerRS in the presence of compound **7** or **8**, we were unable to obtain crystals suitable for high-resolution structure determination. However, we were able to obtain crystals of E. coli SerRS in a co-crystallisation experiment with compound **8, which** was solved at 2.6 Å resolution (**Fig. 2a-b**). The E. coli SerRS-SerSA complex structure was solved in the space group P1 containing two monomers that associate tightly to form a dimer. In contrast, the E. coli SerRS-compound 8 complex structure was solved in space group $P6_122$ with a monomer in the asymmetric unit. We analysed both structures for presence of a second adenylate-binding site as found in the Candida albicans SerRS-SerSA structure (PDB ID: 3QO8)[25]. No density was found in the E. coli SerRS-SerSA structure but some partial density was found in the compound 8 structure, consistent with the observations

found for Candida albicans SerRS, but the lower resolution of our structure and partial occupancy prevent further refinement. Comparison of the structures of E. coli SerRS-SerSA, E. coli SerRS-compound 8, S. aureus SerRS-SerSA and Candida albicans SerRS-SerSA by superimposition shows a significant structural difference in the N-terminal helical arm for tRNA recognition. This suggests that the respective enzymes may have a specific mode of tRNA recognition and binding for proper positioning of the 3'CCA end into the active site (**Supplementary Fig. 5**). Compound **8** binds in a similar fashion to SerSA in E. coli SerRS making all the key interactions with the residues in motif 2, motif 3 and the serine-binding TxE motif as described above. The pyridyl group of compound **8** snuggly fits into the hydrophobic cavity without any other obvious interactions.

Conclusions

In summary, we demonstrate the use of structure-based drug design to identify selective inhibitors of exemplar Seryl-tRNA synthetases from Gram-positive and Gram-negative pathogens on the WHO list of bacteria for which new antibiotics are urgently needed. Previous studies have investigated inhibiting protein synthesis via inhibition of specific aaRS activities leading to the identification of a number of potent antibiotics which have progressed through into clinical studies[21, 26-28]. Rapid development of resistance to these synthetase inhibitors has halted their clinical evaluation[29]. The reported alternative approach herein has been a proof of principle example of the capability of SBDD in modifying a multi-targeting aaRS inhibitor to achieve selectivity.

Further work is required to achieve clinically viable compounds that can permeate the cell membrane but the crystal structures here, nonetheless, provide a foundation for structure-based drug design of novel selective inhibitors which multi-target the aminoacyl tRNA synthetases.

Methods

Synthesis. Full experimental details and characterisation of the compounds are given in Supplementary information.

Protein expression and purification. E. coli SerRS (from E. coli strain B ER2560) and S. aureus SerRS (from S. aureus seg50 (1150)) were cloned into the pET52b(+) vector (Merck Millipore, Germany) using the NcoI and SacI restriction sites allowing for the production of protein with a thrombin cleavable C-terminal His_{10}-tag. E. coli SerRS and S. aureus SerRS were overexpressed in Lemo21(DE3) cells grown in Auto Induction Media – Terrific Broth (Formedium) supplemented with 100 μg/ml ampicillin at 37 °C for 8 hours followed by overnight growth at 25 °C. Cells were harvested by centrifugation at 5000 rpm in a

JLA 8.1000 rotor (Beckman Coulter) for 15 min, and the pellet was re-suspended in buffer A (50 mM Tris, 500 mM NaCl, 30 mM Imidazole, pH 7.5). The cells were disrupted by sonication at 70 % amplitude for 30 sec on ice and 8 pulses. The lysate was centrifuged at 18,000 rpm in a JA 25.50 rotor (Beckman Coulter) for 30 mins. The supernatant was decanted, passed through a 0.2 micron filter and applied to a 5 ml His-Trap column (GE healthcare, USA). The bound protein was eluted with a gradient of buffer B (50 mM Tris, 500 mM NaCl, 500 mM Imidazole, pH 7.5)(0-100% over 50 ml) on an ÄKTA Pure (GE healthcare, USA) at 2 ml/min. The protein SerRS was dialyzed into 2 L of buffer A with thrombin cleavage (1 unit/µg). The protein was passed through the 5 ml His-Trap to remove the cleaved His-Tag and other contaminants. The proteins typically present over 95 % purity at this stage as judged via SDS-PAGE gel and were taken for crystallization trials. Further purification was used for protein used for kinetic and binding studies to ensure complete removal of thrombin using a HiLoad 16/600 Superdex 200 pg column (GE Healthcare, USA) in 20 mM Tris, 200 mM NaCl and 1 mM $MgCl_2$, pH 7.5. The purified protein was subsequently stored in 50 % glycerol at -80 °C.

Crystallisation and structure solution.

Co-crystals of E. coli SerRS in the presence of SerSA were obtained from a drop set up in 96-well sitting drop format with 20 mg ml^{-1} protein and ten-fold molar excess of SerSA. Drops consisted of 100 nl protein preincubated with SerSA and 100 nl reservoir solution with a reservoir volume of 95 ul. Crystals were obtained from a drop containing 0.2 M sodium phosphate monobasic monohydrate, pH 4.7 and 20 % w/v PEG 3350 following incubation at 4 °C and cryoprotected in reservoir solution containing 25 % ethylene glycol.

Co-crystals of His-tagged S. aureus SerRS was obtained from a drop set up with 20 mg ml^{-1} in the presence of ten-fold molar excess of SerSA in 24-well hanging drop format. Drops consisted of 1 µl protein preincubated with SerSA and 1 µl reservoir solution with a reservoir volume of 500 ul. Plates were incubated at 4 °C and crystals obtained in 0.2 M sodium malonate pH 5 and 13 % w/v PEG 3350. Crystals were cryoprotected for 10 s in reservoir solution containing 20 % ethylene glycol and ten-fold molar excess of SerSA.

Crystals of apo-E. coli SerRS were obtained at 21 °C from a 24-well hanging drop format as described above with 30 mg ml^{-1} protein in a crystal condition consisting of 0.1 M sodium citrate pH 5.5, 0.8 M lithium sulfate and 0.05 M ammonium sulfate. A crystal was soaked for 30 mins in 0.1 M sodium citrate pH 5.5, 0.75 M lithium sulfate, 0.05 M ammonium sulfate, 20 % ethylene glycol and 100 mM compound **8** (10 % DMSO in final solution).

All crystals were flash frozen in liquid nitrogen and diffraction data collected at 100 K at beamlines I03 and I04 (Diamond Light Source, United Kingdom). Data was indexed and integrated using iMosflm[30] and scaled using Aimless in CCP4[31] or autoPROC[32] was used in the DLS auto-processing pipeline. The crystal structure of aq_298 (PDB 2DQ3, unpublished) was used as a search model in Phaser MR[33] to solve the structures of E. coli SerRS and S. aureus SerRS by molecular replacement. Refmac5[34] and Phenix[35] were used for iterative rounds of refinement with model building carried out in COOT.[36] Figures were made using PyMOL (Schrödinger, LLC.)

Kinetic analyses. SerRS assays were performed at 37 °C in a Cary 100 UV/Vis double beam spectrophotometer with a thermostatted 6X6 cell changer. The final assay volume was 0.2 ml, containing 50 mM HEPES adjusted to pH 7.6, 10 mM $MgCl_2$, 50 mM KCl, 1 mM dithiothreitol, 10% (v/v) dimethylsulphoxide, 10 mM D-glucose, 0.5 mM NADP+, 1.7 mM.min yeast hexokinase and 0.85 mM.min L. mesenteroides glucose 6-phosphate dehydrogenase. Concentrations of SerRS, amino acid, adenylate (Ap4A) and pyrophosphate were as stated in the text. Unless otherwise stated, background rates were acquired in the absence of amino acid, which was then added to initiate the full reaction. Assays were continuously monitored at 340 nm, to detect reduction of NADP+ to NADPH, where ΔNADPH; 340nm = 6220 M^{-1} cm^{-1}.Kinetic constants relating to substrate dependencies and IC_{50} values for inhibitors were extracted by non-linear regression using GraphPad Prizm 7.00.

Isothermal Titration Calorimetry. Calorimetric titrations of E. coli SerRS with SerSA and/or compound **8** were performed on a VP-ITC microcalorimeter (MicroCal) at 25°C and measured in triplicates. The gel filtration purified E. coli SerRS was concentrated and dialysed overnight against the ITC buffer (20 mM Tris-HCl, pH 7.5 and 200 mM NaCl) at 4°C. All the solutions were degassed by sonication. The overnight dialysis ITC buffer was used to prepare SerSA and compound **8** solutions. The E. coli SerRS (3 µM for SerSA and 7 µM for compound **8**) in the sample cell (1.445 ml) was titrated with ligand solution (70 µM of SerSA and 140 µM of compound **8**) in the syringe (280 ul). The E. coli SerRS - SerSA ITC experiments consisted of a preliminary 2 µl injection followed by 52 successive 5 µl injections. The E. coli SerRS - compound **8** ITC experiments consisted of a preliminary 2 µl injection followed by 26 successive 10 µl injections. Each injection lasted 20 s with an interval of 120 s between consecutive injections. The solution in the reaction cell was stirred at 307 rpm throughout the experiments. The heat response data for the preliminary injection was discarded and the rest of the data was used to generate binding isotherm. The data were fit using either the one binding site model or the two independent binding sites model included in the Origin 7.0 (MicroCal). Thermodynamic parameters, including association constant (K_a), enthalpy (ΔH), entropy (ΔS) and binding stoichiometry (N) were calculated by iterative curve fitting of the binding isotherms. The Gibbs free energy was calculated using $\Delta G = \Delta H - T\Delta S$.

Analytical ultracentrifugation. All experiments were performed at 50000 rpm, using a Beckman Optima analytical ultracentrifuge with an An-50Ti rotor. Data were recorded using the absorbance (at 280 nm with 10 µm resolution and recording scans every 20 seconds) and interference (recording scans every 60 seconds) optical detection systems. The density and viscosity of the buffer was measured experimentally using a DMA 5000M densitometer equipped with a Lovis 200ME viscometer module. The partial specific volume for the protein constructs were calculated using Sednterp from the amino acid sequences. For characterisation of the protein samples, SV scans were recorded for a dilution series, starting from 0.8 mg/mL. Where a ligand was included, this was present at 400 uM (a 20-fold excess over the highest concentration protein sample). Data were processed using SEDFIT, fitting to the c(s) model. Figures were made using GUSSI.

Data availability

The crystallographic data that support the findings of this study are available from the Protein Data Bank (http://www.rcsb.org). E. coli SerRS:SerSA, XXX; S. aureus SerRS:SerSA, XXX; E. coli SerRS:compound **8**, XXX. Additional data that support the findings of this study are available from the corresponding author upon reasonable request.

Acknowledgements

We acknowledge funding from Medical Research Council (MRC) for Innovation Grant MR/M017893/1 and BBSRC Flexible Talent Mobility Account award BB/R506588/1 that supported this work directly and EPSRC AMR bridging the gaps grant EP/M027503/1 that provided initial pump priming activity. We thank Diamond Light Source for beam time (proposal MX14692) and staff at beamlines I03 and I04 for their assistance.

Author contributions

A.J.L, C.G.D, and D.I.R conceived the research. R.C. with the help of C.W.G.F. and L.C. designed, synthesized and characterized compounds used for the study. R.S. produced and purified the enzymes used in biochemical studies. R.S and D.B crystallised the seryl adenylate inhibitors with E. coli SerRS and S. aureus SerRS and collected X-ray data. R.S and A.S.P. solved and refined the crystal structures as presented. R.C with the help of A.J.L. carried out the kinetic studies. R.C, R.S, A.S.P with the help of D.J.S conducted and analysed the results of ITC binding assays, D.J.S and G.M carried out AUC analysis. R.C., R.S. and D.I.R wrote the manuscript. All authors discussed the results and contributed to the final manuscript.

Competing Financial Interests: The authors declare no competing financial interest.

Supplementary Information

Any supplementary information, chemical compound information and source data are available in the online version of the paper.

Table 1: IC_{50} values of designed chemical probes against Seryl-tRNA synthetases. Assays were conducted as reported[6]

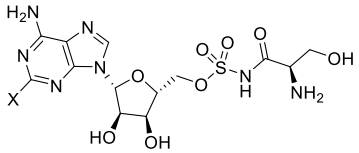

No.	X	IC_{50} E. coli SerRS (µM)	IC_{50} S. aureus SerRS (µM)	IC_{50} Human cytoplasmic SerRS (µM)
1 (Ser)	H	0.21 ± 0.03	0.23 ± 0.49	2.17 ± 0.21
2	Cl	0.45 ± 0.05	0.26 ± 0.03	67.3 ± 4.67
3	I	1.36 ± 0.12	0.38 ± 0.04	24.0 ± 2.26
4	C_6H_5	17.7 ± 1.42	52.7 ± 4.81	>1000 ± >100
5	$_{trans}$-Propenyl	9.38 ± 0.70	3.46 ± 0.47	>1000 ± >100
6	2-Furyl	36.2 ± 2.41	32.4 ± 3.56	>1000 ± >100
7	3-Thienyl	1.44 ± 0.09	1.24 ± 0.12	>1000 ± >100 (ppt)
8	C_5H_4N	6.65 ± 0.64	6.34 ± 0.71	>1000 ± >100 (ppt)

SerRS, Seryl t-RNA synthetase. (ppt) precipitation observed at 1000 µM.
Errors were calculated as s.d. of at least three independent measurements.

Figure 1: Binding mode of SerSA to E. coli and S. aureus SerRS. a: Superposition of E. coli SerRS (blue) and S. aureus SerRS (gold) with SerSA bound (boxed). **b**: Interactions of SerSA (green sticks) with E. coli SerRS chain A. Water represented as a red sphere. Hydrogen bond interactions shown as black dashes. **c**: Interactions of SerSA with S. aureus SerRS.

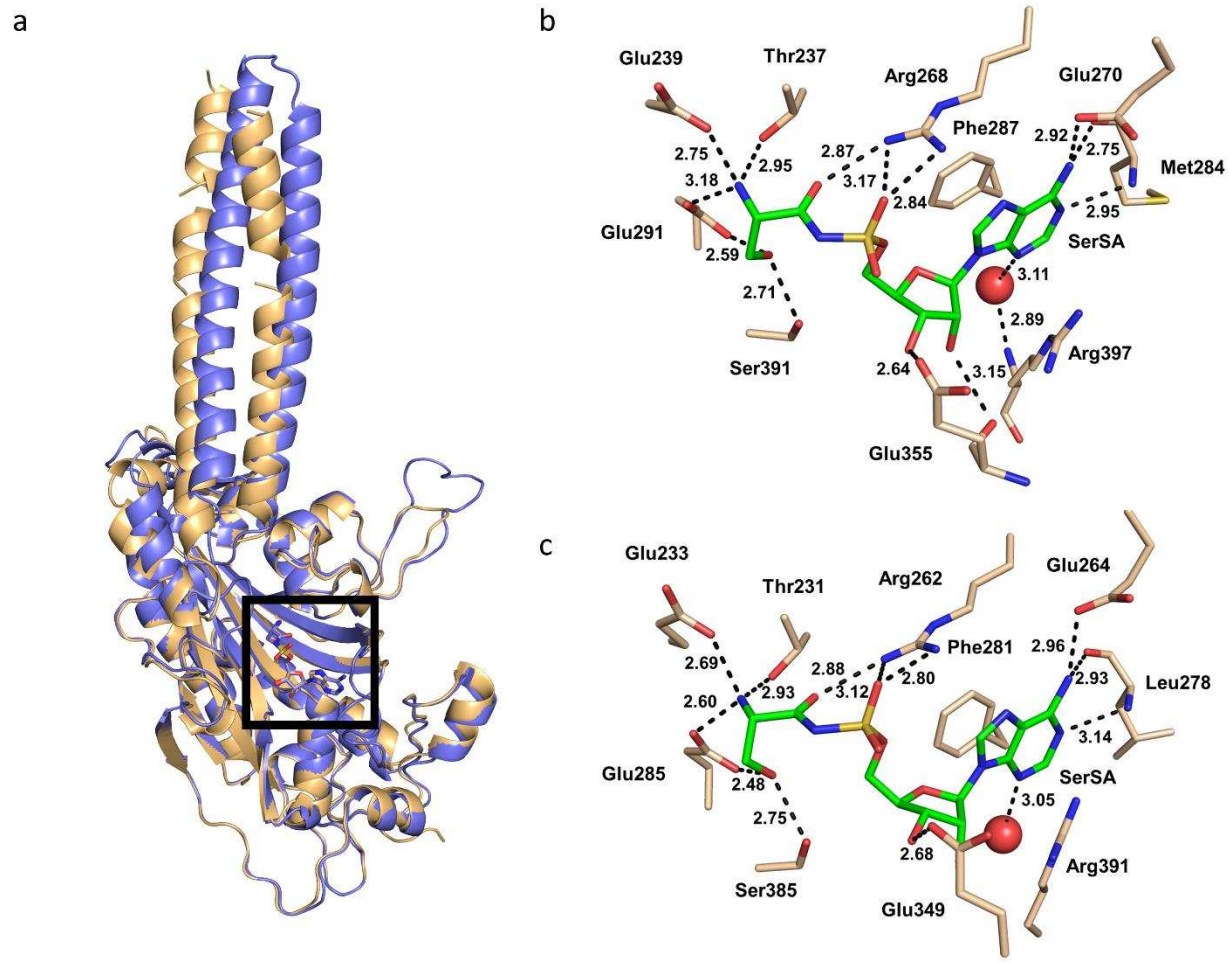

Figure 2: Comparison of binding of SerSA and compound 8 to E. coli SerRS. a: The chemical structures of the compounds used in this study. **b**: Pyridyl group of compound 8 (boxed) positioned in active site. **c**: Interactions of compound 8 (green sticks) with E. coli SerRS. Hydrogen bond interactions are shown as black dashes. d: Superposition of E. coli SerRS:SerSA (blue) with E. coli SerRS:compound 8.

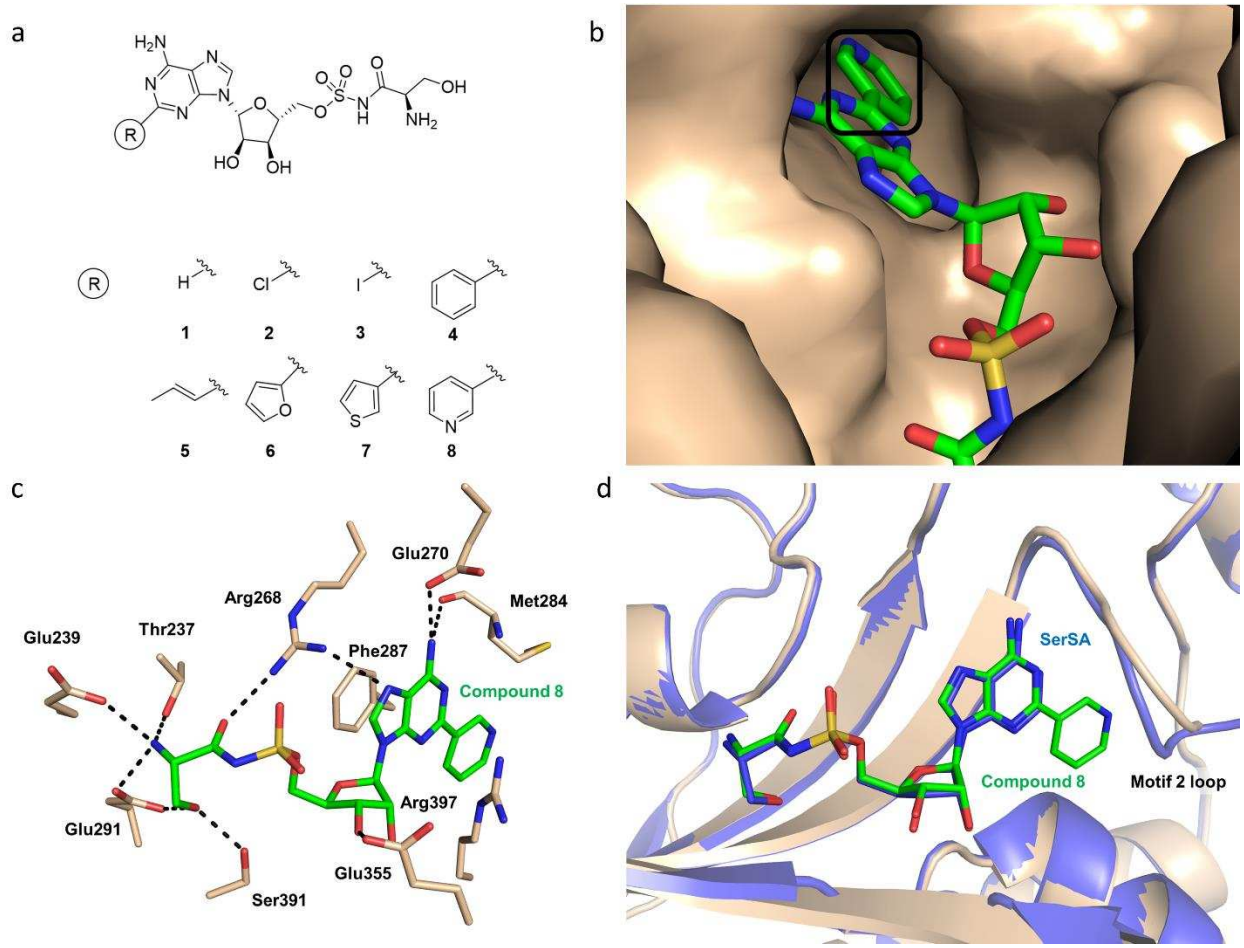

References

1. Lenhard, B., Orellana, O., Ibba, M. & Weygand-Durasevic, I. tRNA recognition and evolution of determinants in seryl-tRNA synthesis. *Nucleic Acids Research* **27**, 721-729 (1999).
2. F C Neidhardt, J Parker, a. & McKeever, W.G. Function and Regulation of Aminoacyl-tRNA Synthetases in Prokaryotic and Eukaryotic Cells. *Annual Review of Microbiology* **29**, 215-250 (1975).
3. Schimmel, P., Tao, J. & Hill, J. Aminoacyl tRNA synthetases as targets for new anti-infectives. *FASEB J* **12**, 1599-1609 (1998).
4. Ho, J.M., Bakkalbasi, E., Soll, D. & Miller, C.A. Drugging tRNA aminoacylation. *RNA Biol* **15**, 667-677 (2018).
5. Ataide, S.F. & Ibba, M. Small molecules: big players in the evolution of protein synthesis. *ACS Chem Biol* **1**, 285-297 (2006).
6. Lloyd, A.J., Potter, N.J., Fishwick, C.W.G., Roper, D.I. & Dowson, C.G. Adenosine Tetraphosphoadenosine Drives a Continuous ATP-Release Assay for Aminoacyl-tRNA Synthetases and Other Adenylate-Forming Enzymes. *ACS Chemical Biology* **8**, 2157-2163 (2013).
7. Cvetesic, N. & Gruic-Sovulj, I. Synthetic and editing reactions of aminoacyl-tRNA synthetases using cognate and non-cognate amino acid substrates. *Methods* **113**, 13-26 (2017).
8. Perona, J.J. & Gruic-Sovulj, I. Synthetic and editing mechanisms of aminoacyl-tRNA synthetases. *Top Curr Chem* **344**, 1-41 (2014).
9. Dewan, V., Reader, J. & Forsyth, K.M. Role of aminoacyl-tRNA synthetases in infectious diseases and targets for therapeutic development. *Top Curr Chem* **344**, 293-329 (2014).
10. Van de Vijver, P. *et al.* Antibacterial 5'-O-(N-dipeptidyl)-sulfamoyladenosines. *Bioorganic & Medicinal Chemistry* **17**, 260-269 (2009).
11. Silvian, L.F., Wang, J. & Steitz, T.A. Insights into editing from an ile-tRNA synthetase structure with tRNAile and mupirocin. *Science* **285**, 1074-1077 (1999).
12. Guo, M. *et al.* Paradox of mistranslation of serine for alanine caused by AlaRS recognition dilemma. *Nature* **462**, 808-812 (2009).
13. Cusack, S., Berthet-Colominas, C., Hartlein, M., Nassar, N. & Leberman, R. A second class of synthetase structure revealed by X-ray analysis of Escherichia coli seryl-tRNA synthetase at 2.5 A. *Nature* **347**, 249-255 (1990).
14. Belrhali, H. *et al.* Crystal structures at 2.5 angstrom resolution of seryl-tRNA synthetase complexed with two analogs of seryl adenylate. *Science* **263**, 1432-1436 (1994).
15. Fujinaga, M., Berthet-Colominas, C., Yaremchuk, A.D., Tukalo, M.A. & Cusack, S. Refined crystal structure of the seryl-tRNA synthetase from Thermus thermophilus at 2.5 A resolution. *J Mol Biol* **234**, 222-233 (1993).
16. Bilokapic, S. *et al.* Structure of the unusual seryl-tRNA synthetase reveals a distinct zinc-dependent mode of substrate recognition. *EMBO J* **25**, 2498-2509 (2006).
17. Itoh, Y. *et al.* Crystallographic and mutational studies of seryl-tRNA synthetase from the archaeon Pyrococcus horikoshii. *RNA Biol* **5**, 169-177 (2008).
18. Rocha, R., Pereira, P.J., Santos, M.A. & Macedo-Ribeiro, S. Unveiling the structural basis for translational ambiguity tolerance in a human fungal pathogen. *Proc Natl Acad Sci U S A* **108**, 14091-14096 (2011).
19. Xu, X., Shi, Y. & Yang, X.L. Crystal structure of human Seryl-tRNA synthetase and Ser-SA complex reveals a molecular lever specific to higher eukaryotes. *Structure* **21**, 2078-2086 (2013).
20. Chimnaronk, S., Gravers Jeppesen, M., Suzuki, T., Nyborg, J. & Watanabe, K. Dual-mode recognition of noncanonical tRNAs(Ser) by seryl-tRNA synthetase in mammalian mitochondria. *EMBO J* **24**, 3369-3379 (2005).

21. Brown, M.J.B. *et al.* Rational Design of Femtomolar Inhibitors of Isoleucyl tRNA Synthetase from a Binding Model for Pseudomonic Acid-A. *Biochemistry* **39**, 6003-6011 (2000).
22. Miyaura, N., Yamada, K. & Suzuki, A. A new stereospecific cross-coupling by the palladium-catalyzed reaction of 1-alkenylboranes with 1-alkenyl or 1-alkynyl halides. *Tetrahedron Letters* **20**, 3437-3440 (1979).
23. Srikrishna, A., Viswajanani, R., Sattigeri, J.A. & Vijaykumar, D. A new, convenient reductive procedure for the deprotection of 4-methoxybenzyl (MPM) ethers to alcohols. *The Journal of Organic Chemistry* **60**, 5961-5962 (1995).
24. Cusack, S., Hartlein, M. & Leberman, R. Sequence, structural and evolutionary relationships between class 2 aminoacyl-tRNA synthetases. *Nucleic Acids Res.* **19**, 3489-3498 (1991).
25. Rocha, R., Pereira, P.J.B., Santos, M.A.S. & Macedo-Ribeiro, S. Unveiling the structural basis for translational ambiguity tolerance in a human fungal pathogen. *Proceedings of the National Academy of Sciences* **108**, 14091-14096 (2011).
26. Wu, Y. *et al.* Potent and selective inhibitors of Staphylococcus epidermidis tryptophanyl-tRNA synthetase. *Journal of Antimicrobial Chemotherapy* **60**, 502-509 (2007).
27. Kim, S.Y., Lee, Y.-S., Kang, T., Kim, S. & Lee, J. Pharmacophore-based virtual screening: The discovery of novel methionyl-tRNA synthetase inhibitors. *Bioorganic & Medicinal Chemistry Letters* **16**, 4898-4907 (2006).
28. Teng, M. *et al.* Identification of Bacteria-Selective Threonyl-tRNA Synthetase Substrate Inhibitors by Structure-Based Design. *Journal of Medicinal Chemistry* **56**, 1748-1760 (2013).
29. Hernandez, V. *et al.* Discovery of a novel class of boron-based antibacterials with activity against gram-negative bacteria. *Antimicrob Agents Chemother* **57**, 1394-1403 (2013).
30. Battye, T.G., Kontogiannis, L., Johnson, O., Powell, H.R. & Leslie, A.G. iMOSFLM: a new graphical interface for diffraction-image processing with MOSFLM. *Acta Crystallogr D Biol Crystallogr* **67**, 271-281 (2011).
31. Winn, M.D. *et al.* Overview of the CCP4 suite and current developments. *Acta Crystallogr D Biol Crystallogr* **67**, 235-242 (2011).
32. Vonrhein, C. *et al.* Data processing and analysis with the autoPROC toolbox. *Acta Crystallogr D Biol Crystallogr* **67**, 293-302 (2011).
33. McCoy, A.J. *et al.* Phaser crystallographic software. *Journal of Applied Crystallography* **40**, 658-674 (2007).
34. Murshudov, G.N., Vagin, A.A. & Dodson, E.J. Refinement of macromolecular structures by the maximum-likelihood method. *Acta Crystallogr D Biol Crystallogr* **53**, 240-255 (1997).
35. Adams, P.D. *et al.* PHENIX: a comprehensive Python-based system for macromolecular structure solution. *Acta Crystallogr D Biol Crystallogr* **66**, 213-221 (2010).
36. Emsley, P., Lohkamp, B., Scott, W.G. & Cowtan, K. Features and development of Coot. *Acta Crystallographica Section D* **66**, 486-501 (2010).